Variational approach to nonlinear pulse propagation in optical fibers

D. Anderson
Institute for Electromagnetic Field Theory and EURATOM Fusion Research (EUR-EFN), Chalmers University of Technology, S-412 96 Göteborg, Sweden
(Received 28 January 1983)

The problem of nonlinear pulse propagation in optical fibers, as governed by the nonlinear Schrödinger equation, is reformulated as a variational problem. By means of Gaussian trial functions and a Ritz optimization procedure, approximate solutions are obtained for the evolution during propagation of pulse width, pulse amplitude, and nonlinear frequency chirp. Comparisons with results from inverse-scattering theory and/or numerically obtained solutions show very good agreement.

I. INTRODUCTION

Interest in nonlinear properties of short-pulse propagation in optical fibers has grown tremendously during the last few years.[1–6] The two main reasons for this interest are (i) the possibility of undistorted optical-pulse propagation offered by soliton pulses[1–4] and (ii) the possibility of extreme compression of optical pulses resulting in pulse widths well into the femtosecond domain.[1,5,6]

An important limiting factor in the development towards high data-transmission rates in long optical fibers is the inherent dispersive pulse broadening effect.[3] It was suggested already, in 1973 by Hasegawa and Tappert,[7] that it should be possible to balance the dispersive spreading of an optical pulse by a pulse-narrowing effect associated with the weak nonlinearity of the index of refraction in the fiber. However, at that time there existed neither fibers with sufficiently low loss nor lasers at the appropriate wavelengths to verify the theoretical predictions.

The subsequent explosive growth in optical-fiber technology has led to single-mode fibers with extremely low losses (less than 1 dB/km) and to lasers with wavelengths in the range where the group-velocity dispersion becomes negative (a necessary condition for soliton pulse propagation).

In 1980, the first experimental observation of solitons in optical fibers was made.[1] In a remarkably conclusive experiment several of the characteristic soliton properties were verified. In particular, undistorted pulse propagation over long distance was demonstrated for situations where the dispersive pulse spreading was exactly balanced by nonlinear pulse-narrowing effects. In addition, the pulse compression and pulse-splitting characteristic of higher-order soliton solutions were also observed and found to be in excellent agreement with theoretical predictions.

Following the feasibility demonstration implied by this experiment, a sequence of papers have investigated different aspects of nonlinear short-pulse propagation in long optical fibers. A major effort has been concentrated on the possibility of creating extremely short optical pulses in situations where the nonlinear compressional effects dominate the dispersive spreading.

In a series of experiments,[5,8] Grischkowsky and co-workers have achieved optical-pulse compression factors of 10–12 resulting in subpicosecond pulses. Unprecedented to date is the 30 fsec pulses reported by Shank *et al.*[6] also obtained using optical nonlinear compression techniques.

The theoretical foundation for the analysis of nonlinear pulse propagation in optical fibers is the nonlinear Schrödinger equation (NLS) (Refs. 1–8), which governs the evolution of the pulse envelope. This equation can, in principle, be solved exactly using inverse-scattering technique.[9] However, the corresponding solutions, albeit exact, are not very explicit, except for the special cases of the soliton solutions. The lowest-order soliton corresponds to an input of hyberbolic secant shape and propagates with unchanged form along the fiber. Higher-order solitons have amplitudes being integer multiples of the fundamental soliton amplitude and exhibit a more complicated amplitude variation involving periodic pulse narrowing and pulse splitting.

In addition to these so-called "bright" soliton solutions,[7] which require anomalous net dispersion properties, there also exist "dark" soliton solutions of hyperbolic tangent shape,[7] when net dispersion is normal. (Normal dispersion is defined by $\partial v_g/\partial k < 0$, where v_g is the group velocity and k is the wave number of the wave.) The technical importance of this situation for pulse compression has been amply demonstrated in Refs. 5, 6, and 8, where the combined action of fiber dispersion and nonlinearity has been used to create strongly frequency chirped optical pulses. The pulses are subsequently passed either through a sodium-vapor cell[5,8] or a grating compressor,[6] where linear dispersion compresses the pulses in a way analogous to the chirp radar compression scheme.

The complicated form of the exact solution for the NLS has motivated many numerical investigations[9] as a complementary tool towards the understanding of the properties of the NLS. In view of this, it would also be very desirable to obtain approximate analytical results giving some of the most important features of the solutions as, e.g., the pulse compression factor. Obviously, this cannot be done without sacrificing some of the more detailed information of the solutions. On the other hand, approximate solutions could prove very useful for applications as well as for providing a better physical understanding of the interplay between dispersion and nonlinear effects in connection with pulse propagation in optical fibers.

In the present work we will employ a variational approach involving trial functions in order to describe the main characteristics of the pulse evolution as determined by the NLS. This approach has previously been used to investigate the related problem of nonlinear self-focusing of laser beams,[10,11] where good agreement with numerical results has been obtained. The main advantage of the variational approach in the present context is that it provides explicit, although approximate, analytical expressions for the pulse compression/decompression factor, the maximum pulse amplitude, and the induced frequency chirp. These are the three most important single parameters characterizing the pulse evolution.

The main shortcoming of the use of trial functions is the inability to account for changes in pulse shape. Thus, if we use a Gaussian trial function, its amplitude, width, frequency, etc., may be allowed to vary, but the Gaussian pulse shape is assumed to be inherently preserved. However, changes in shape do play an important role in several circumstances. The pulse-compression technique demonstrated by Grischkowsky *et al.*,[5,8] uses the deformation of the pulse towards a rectangular shape. This form has the advantage of creating a linear frequency chirp through nonlinear self-phase modulation. The subsequent dispersive pulse compression then results in a pulse with strongly reduced wings. Furthermore, effects like the higher-order soliton splitting[1] are obviously out of reach in the present analysis and will only be indicated as a pulse broadening.

With these caveats in mind, the present approach, on one hand, gives useful approximate expressions for the evolution of characteristic pulse parameters like the compression factor, the amplitude, and the nonlinearly induced frequency chirp and, on the other hand, provides a suggestive description of the complicated interplay between dispersive and nonlinear effects.

II. THE NONLINEAR SCHRÖDINGER EQUATION

In a nonlinear optical medium with a cubic nonlinearity, the index of refraction n is given by

$$n=n_0(\omega)+n_2\langle E^2\rangle \ , \tag{1}$$

where $n_0(\omega)$ represents the linear part and n_2 determines the nonlinear change in the refractive index due to the presence of the wave. The optical wavefield $E(r,x,t)$ is taken as[3]

$$E(r,x,t)=\mathrm{Re}\{\psi(x,t)R(r)\exp[i(k_0x-\omega_0t)]\} \ , \tag{2}$$

where $\psi(x,t)$ is a slowly varying function of time t and x, the coordinate along the fiber. $R(r)$ is the linear radial eigenfunction of the mode, and k_0 and ω_0 are the wave number and the frequency of the wave $[k_0=n_0(k_0)\omega_0/c]$. The use of the linear eigenmode for the radial dependence is motivated by the fact that the intensities considered in the present context are far below the threshold for nonlinear self-focusing.[3] Assuming that the nonlinear and dispersive effects are weak, and averaging $R(r)$ over the cross section of the fiber, one obtains[3]

$$i\left[\frac{\partial\psi}{\partial x}+k_0'\frac{\partial\psi}{\partial t}\right]-\tfrac{1}{2}k_0''\frac{\partial^2\psi}{\partial t^2}+\frac{\omega_0 n_2}{4c}\,|\psi|^2\psi=0 \ , \tag{3}$$

where

$$k_0'=[\partial k(\omega)/\partial\omega]_{\omega=\omega_0} \ ,$$

$$k_0''=[\partial^2 k(\omega)/\partial\omega^2]_{\omega=\omega_0} \ ,$$

and c is the velocity of light. Finally, we introduce the convenient variable $\tau=t-k_0'x$ and arrive at the nonlinear Schrödinger equation

$$i\frac{\partial\psi}{\partial x}=\alpha\frac{\partial^2\psi}{\partial\tau^2}+\kappa\,|\psi|^2\psi \ , \tag{4}$$

where $\alpha=\frac{1}{2}k_0''$ and $\kappa=-\omega_0n_2/4c$. Particular solutions of Eq. (4) have been found,[7] the simplest ones being the single bright soliton solution $(\kappa/\alpha>0)$

$$\psi=\rho_0[\mathrm{sech}(\tau/\tau_b)]e^{i\lambda_b x} \ , \tag{5}$$

where

$$\frac{1}{\tau_b}=\rho_0(\kappa/2\alpha)^{1/2} ,$$
$$\lambda_b=-(\kappa/2)\rho_0^2 , \tag{6}$$

and the corresponding dark soliton solution ($\kappa/\alpha<0$)

$$\psi=\rho_0[\tanh(\tau/\tau_d)]e^{i\lambda_d x} , \tag{7}$$

where

$$\frac{1}{\tau_d}=\rho_0\left|\frac{\kappa}{2\alpha}\right|^{1/2} ,$$
$$\lambda_d=-\kappa\rho_0^2 . \tag{8}$$

Pulses of the form given by Eqs. (5) and (7), with parameters related by Eqs. (6) and (8), respectively, will propagate along the optical fiber with preserved shape as a result of an exact balance between dispersive and nonlinear effects. However, if the soliton parameters are not related by Eqs. (6) and (8), the pulse form will change in a complicated way, which is not easily described analytically. It has been shown numerically[9] for the case $\kappa/\alpha>0$ that if the soliton width τ_b in Eq. (5) is kept fixed, and ρ_0 takes on values being integer multiples of the fundamental soliton amplitude $(2\alpha/\kappa)^{1/2}/\tau_b$, higher-order solitons are obtained. These exhibit successively more complicated oscillatory behavior involving pulse compression/decompression and pulse splitting.

For amplitudes, which are not exact integer multiples of the fundamental amplitude, the pulse will oscillatively change shape and asymptotically settle down to the N-soliton solution corresponding to the closest integer.[3,9] Actually, inverse-scattering theory predicts that any reasonable initial pulse shape will eventually produce a discrete N-soliton solution when the continuous "excess modes" have died away.

In the present work, we will give an approximate description of the evolution of some of the most fundamental properties connected with the nonlinear propagation of optical pulses. In particular, we will concentrate on information concerning pulse width, pulse amplitude, and frequency chirp. For this purpose we will, in the next section, reformulate the NLS equation as a variational problem.

III. A VARIATIONAL FORMULATION OF THE NLS EQUATION

Our approximate analysis of the pulse propagation problem will involve essentially a Ritz optimization procedure,[10,11] based on the variational functional corresponding to the NLS equation. It is easily shown that the NLS equation [Eq. (4)] can be restated as a variational problem corresponding to the Lagrangian L given by

$$L=\frac{i}{2}\left[\psi\frac{\partial\psi^*}{\partial x}-\psi^*\frac{\partial\psi}{\partial x}\right]-\alpha\left|\frac{\partial\psi}{\partial\tau}\right|^2+\frac{\kappa}{2}|\psi|^4 , \tag{9}$$

where the asterisk denotes the complex conjugate. This implies that the NLS equation results from the variational equations corresponding to the variational principle

$$\delta\int\int L\left[\psi,\psi^*,\frac{\partial\psi}{\partial x},\frac{\partial\psi^*}{\partial x},\frac{\partial\psi}{\partial\tau},\frac{\partial\psi^*}{\partial\tau}\right]dx\,d\tau=0 , \tag{10}$$

i.e., the equation

$$\frac{\delta L}{\delta\psi^*}=\frac{\partial}{\partial x}\frac{\partial L}{\partial\left[\dfrac{\partial\psi^*}{\partial x}\right]}+\frac{\partial}{\partial\tau}\frac{\partial L}{\partial\left[\dfrac{\partial\psi^*}{\partial\tau}\right]}-\frac{\partial L}{\partial\psi^*}=0 \tag{11}$$

is equivalent to Eq. (4).

In the Ritz optimization procedure, the first variation of the variational functional is made to vanish within a set of suitably chosen trial functions. As trial functions we will use Gaussian shaped pulses. This choice is convenient but by no means the only possible one e.g., hyperbolic secant shaped pulses would have done equally well, and for some situations even better. The only advantage of the Gaussian shaped pulse is that in the linear limit the variational equations will reproduce the exact solution of Eq. (4). Thus, we assume that the initial pulse has a Gaussian form or a shape which can reasonably well be approximated by a Gaussian, i.e.,

$$\psi(0,\tau)=A_0\exp\left[-\frac{\tau^2}{2a_0^2}\right] , \tag{12}$$

where A_0 is the maximum amplitude of the pulse and a_0 is the characteristic pulse width.

The subsequent evolution of the pulse envelope for $x>0$ is assumed to be describable as [cf. Eqs. (5) and (7)]

$$\psi(\tau,x)=A(x)\exp\left[-\frac{\tau^2}{2a^2(x)}+ib(x)\tau^2\right] , \tag{13}$$

i.e., as a still Gaussian shaped pulse, where the (complex) amplitude $A(x)$, the pulse width $a(x)$, and the frequency chirp $2b(x)\tau$ all are allowed to vary with distance of propagation.

Inserting the trial function given by Eq. (13) into the variational principle, Eq. (10), we obtain the reduced variational problem

$$\delta \int \langle L \rangle dx = 0 \,, \tag{14}$$

where

$$\langle L \rangle = \int_{-\infty}^{+\infty} L_G d\tau \,, \tag{15}$$

and L_G denotes the result of inserting the Gaussian ansatz into the Lagrangian L. By performing the integration implied by Eq. (15) we obtain

$$\langle L \rangle = \frac{\sqrt{\pi}}{2} \left[ia \left[A\frac{dA^*}{dx} - A^*\frac{dA}{dx} \right] + |A|^2 a^3 \frac{db}{dx} - \alpha a^3 |A|^2 \left[4b^2 + \frac{1}{a^4} \right] + \frac{1}{\sqrt{2}} \kappa a |A|^4 \right] . \tag{16}$$

The reduced variational principle, expressed by Eq. (14), results in a set of coupled ordinary differential equations for the Gaussian parameters A, a, and b, which together determines the evolution of the pulse.

IV. VARIATIONAL EQUATIONS FOR THE GAUSSIAN PARAMETERS

We can now proceed to study the variational equations for the Gaussian parameter functions $A(x)$, $A^*(x)$, $a(x)$, and $b(x)$ which result from the variational principle [Eq. (14)] with the reduced Lagrangian $\langle L \rangle$ given by Eq. (16). The following variational equations are obtained:

$$\frac{\delta\langle L \rangle}{\delta A^*} = 0 \Longrightarrow \frac{d}{dx}(iaA) = -ia\frac{dA}{dx} + Aa^3\frac{db}{dx} - \alpha a^3 A \left[4b^2 + \frac{1}{a^4} \right] + \sqrt{2}\kappa a |A|^2 A \,, \tag{17}$$

$$\frac{\delta\langle L \rangle}{\delta A} = 0 \Longrightarrow \frac{d}{dx}(-iaA^*) = -ia\frac{dA^*}{dx} + A^* a^3\frac{db}{dx} - \alpha a^3 A^* \left[4b^2 + \frac{1}{a^4} \right] + \sqrt{2}\kappa a |A|^2 A \,, \tag{18}$$

$$\frac{\delta\langle L \rangle}{\delta a} = 0 \Longrightarrow i \left[A\frac{dA^*}{dx} - A^*\frac{dA}{dx} \right] + 3|A|^2 a^2 \frac{db}{dx} - 6\alpha a^2 b^2 + \alpha\frac{|A|^2}{a^2} + \frac{1}{\sqrt{2}}\kappa |A|^4 = 0 \,, \tag{19}$$

$$\frac{\delta\langle L \rangle}{\delta b} = 0 \Longrightarrow \frac{d}{dx}(a^3|A|^2) = -4\alpha b a^3 |A|^2 \,. \tag{20}$$

If we multiply Eqs. (17) and (18) with A^* and A, respectively, we obtain by subtracting and adding the following equations:

$$\frac{d}{dx}(a|A|^2) = 0 \,, \tag{21}$$

$$i\left[A^*\frac{dA}{dx} - A\frac{dA^*}{dx} \right] = |A|^2 \left[a^2\frac{db}{dx} - \alpha a^2 \left[4b^2 + \frac{1}{a^4} \right] + \sqrt{2}\kappa |A|^2 \right] . \tag{22}$$

Equation (21) implies a constant of motion, i.e.,

$$a(x)|A(x)|^2 = \text{const} = a_0|A_0|^2 = E_0 \,, \tag{23}$$

which expresses the fact that the energy of the pulse does not change. This result could also have been obtained from the well-known invariant of the NLS equation, viz.,

$$\int_{-\infty}^{+\infty} |\psi(x,\tau)|^2 d\tau = \text{const} \,. \tag{24}$$

Using the fact that $a(x)|A(x)|^2$ is constant, we obtain from Eq. (20)

$$\frac{da}{dx} = -4\alpha ab \,. \tag{25}$$

By comparing Eqs. (19) and (22) we have

$$a\frac{db}{dx} - 4\alpha ab^2 + \frac{\alpha}{a^3} - \frac{\kappa}{2\sqrt{2}}\frac{|A|^2}{a} = 0 \,, \tag{26}$$

which can be combined with the derivative form of Eq. (25) to yield

$$\frac{d^2a}{dx^2} = \frac{4\alpha^2}{a^3} - \alpha\kappa\sqrt{2}\frac{|A|^2}{a} \,. \tag{27}$$

We finally eliminate $|A|^2$ by means of the constant of motion, Eq. (23), and integrate Eq. (27) once.

This yields an equation for the variation of $a(x)$, which is analogous to that of a particle moving in a potential well, viz.,

$$\frac{1}{2}\left[\frac{da}{dx}\right]^2+\Pi(a)=0 . \tag{28}$$

The potential field $\Pi(a)$ is given by

$$\Pi(a)=\frac{2\alpha^2}{a^2}-\alpha\kappa\sqrt{2}\frac{E_0}{a}+c , \tag{29}$$

where c is a constant to be determined by initial conditions.

Thus, the solution of the variational problem is reduced to solving Eq. (28) for the pulse width variation, since once $a(x)$ is known, the frequency chirp parameter $b(x)$ is determined by Eq. (25) as

$$b(x)=-\frac{1}{4\alpha}\frac{d\ln a}{dx} \tag{30}$$

and the absolute value of the amplitude $|A(x)|$ is determined by the constant of motion, Eq. (23). Finally the phase $\phi(x)$ of $A(x)$ (writing $A(x)=|A(x)|\exp[i\phi(x)]$) is obtained from Eq. (22), using also Eq. (26)

$$\frac{d\phi}{dx}=\frac{\alpha}{a^2}-\frac{5\sqrt{2}}{8}\kappa|A|^2 . \tag{31}$$

The potential well description for the variation of $a(x)$, as given by Eqs. (28) and (29), conveys a suggestive physical picture of the competition between dispersive and nonlinear effects. This will be discussed in more detail in the next section.

V. THE POTENTIAL WELL DESCRIPTION

For the further analysis of Eqs. (28) and (29), describing the evolution of the pulse width, it is convenient to introduce the normalization $a(x)/a_0=y(x)$ and the constants

$$\mu=\frac{2\alpha^2}{a_0^4}>0 ,$$
$$\nu=\sqrt{2}\frac{\alpha\kappa E_0}{a_0^3} , \tag{32}$$
$$K=\frac{c}{a_0^2} .$$

This yields

$$\frac{1}{2}\left[\frac{dy}{dx}\right]^2+\Pi(y)=0 \tag{33}$$

with

$$\Pi(y)=\frac{\mu}{y^2}+\frac{\nu}{y}+K . \tag{34}$$

We assume that the "particle starts from rest," i.e., that the pulse at $x=0$ has $a(0)=a_0$ and $[da(x)/dx]_{x=0}=0$. This determines K to be

$$K=-(\mu+\nu) . \tag{35}$$

The characteristic behavior of $a(x)$ can very conveniently be inferred from the properties of the potential function $\Pi(y)$. We will begin this study by first considering the linear limit, i.e., $\kappa=0$ which implies $\nu=0$.

A. Linear theory

In the limit when only linear dispersion is operative, the potential function becomes

$$\Pi(y)=\frac{\mu}{y^2}-\mu \tag{36}$$

and the general form of $\Pi(y)$ is given in Fig. 1. The mechanical analogy implies that a particle released from rest at $y=1$ will move towards larger y and descend the potential slope with ever increasing speed. This obviously corresponds to the ordinary monotonous dispersive spreading of a wave pulse in a dispersive medium. The analysis can be made more quantitative by solving Eq. (31) for the variation of $a(x)$. This directly yields

$$y^2(x)=1+2\mu x^2=1+\frac{4\alpha^2x^2}{a_0^4} . \tag{37}$$

From Eq. (30) we obtain

$$b(x)=-\frac{\alpha x/a_0^2}{a_0^2(1+4\alpha^2x^2/a_0^4)} . \tag{38}$$

The variation of $|A(x)|$ is found from Eq. (23)

$$|A(x)|=|A_0|\left[1+4\frac{\alpha^2x^2}{a_0^4}\right]^{-1/4} , \tag{39}$$

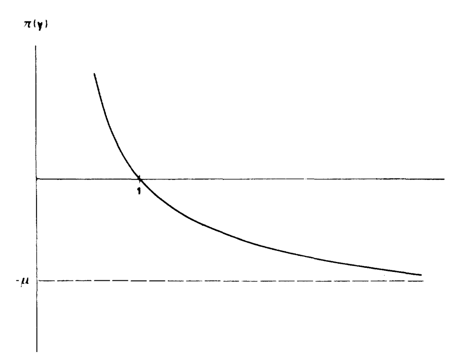

FIG. 1. Qualitative plot of the potential function $\Pi(y)$ in the linear case ($\nu=0$).

and the phase variation $\phi(x)$ is determined from Eq. (31) as

$$\phi(x)=\tfrac{1}{2}\arctan\frac{2\alpha x}{a_0^2}\ . \tag{40}$$

The solution given by Eqs. (37)–(40) is more than an approximate solution; it coincides with the exact solution for the well-known dispersive spreading of a Gaussian pulse, viz.,

$$\psi(x,\tau)=|A_0|\left[1-\frac{2i\alpha x}{a_0^2}\right]^{1/2}\times\exp\left[-\frac{\tau^2}{2a_0^2(1-2i\alpha x/a_0^2)}\right]. \tag{41}$$

This result gives an indication of the power of approximation of the variational approach.

B. Qualitative nonlinear theory

The dynamic interplay between dispersion and nonlinearity is reflected in the properties of the potential function which turn out to depend crucially on the sign and magnitude of the ratio ν/μ, i.e., on the relative importance of dispersion and nonlinearity. The following properties are sufficient to understand the qualitative behavior of $\Pi(y)$:

(i) $\Pi(y)\rightarrow\begin{cases}\infty, & y\rightarrow 0\\ -(\mu+\nu), & y\rightarrow\infty\end{cases}$

(ii) $\Pi(y)=0$ for $y=1$ and $y=-(1+\nu/\mu)^{-1}\equiv y_*$,

(iii) $\Pi'(y)=0$ for $y=y_m=-2\mu/\nu$,

(iv) $\Pi'(1)=-\mu(2+\nu/\mu)$,

(v) $\Pi(y_m)=-(2\mu+\nu)^2/(4\mu)\leq 0$.

These results imply that it is convenient to divide the possible values of ν/μ into four distinct regions, characterized by very different properties.

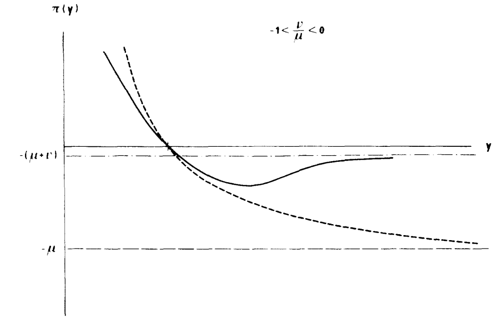

FIG. 3. Qualitative plot of the potential function $\Pi(y)$ in the case of anomalous dispersion and weak nonlinearity $(-1<\nu/\mu<0)$. For comparison the linear case is also inserted (— — —).

Region I: $\nu/\mu>0$ (normal dispersion, $\alpha/\kappa<0$). The qualitative behavior of $\Pi(y)$ in this region is shown in Fig. 2. The potential curve is found to lie below that of the linear case for $y>1$. The physical inference is that the nonlinearity increases the pulse spreading, making the pulse broaden at a faster rate than in the purely linear case.

Region II: $-1<\nu/\mu>0$ (anomalous dispersion, $\alpha/\kappa<0$, and weak nonlinearity). A qualitative plot of $\Pi(y)$ for this range of values is shown in Fig. 3. The nonlinearity is seen to oppose the dispersive spreading of the pulse, but is not strong enough to cancel the linear pulse broadening effect.

Region III: $-2<\nu/\mu<-1$ (anomalous dispersion, $\alpha/\kappa>0$, and intermediately strong nonlinearity). From Fig. 4, we see that the nonlinearity is now strong enough to create a potential well between $y=1$ and $y=y_*\equiv-(1+\nu/\mu)^{-1}$. A mechanical analogy suggests a solution which oscillates between the zeros of $\Pi(y)$. Thus, in this case, the dispersive

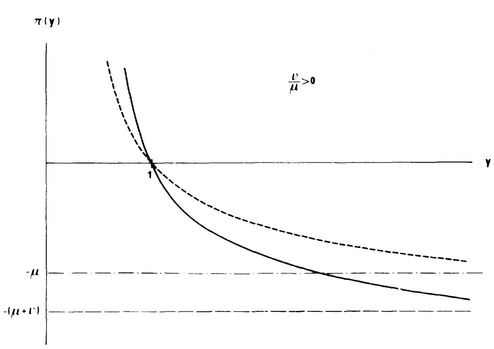

FIG. 2. Qualitative plot of the potential function $\Pi(y)$ in the case of normal dispersion $(\nu/\mu>0)$. For comparison the linear case is also inserted (— — —).

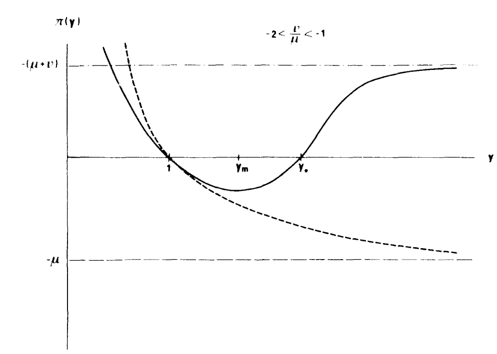

FIG. 4. Qualitative plot of the potential function $\Pi(y)$ in the case of anomalous dispersion and intermediately strong nonlinearity $(-2<\nu/\mu<-1)$. For comparison the linear case is also inserted (— — —).

spreading of the pulse is stopped at $y=y_*$ by nonlinear effects, which subsequently compress the pulse back to the initial pulse width. This behavior is repeated in an oscillatory manner.

Limit case. $\nu/\mu=-2$. In the limit, when $\nu/\mu\to-2$, we obtain $y_*=1=y_m$ and $\Pi'(1)=0=\Pi(y_m)$. The potential well has degenerated into a single point and a particle released at this point will stay there. In the present context, this implies that a wave pulse for which $\nu/\mu=-2$ propagates with unchanged form as a consequence of an exact balance between nonlinear and dispersive effects. This should correspond to the case of a bright soliton solution. The condition $\nu/\mu=-2$ translates into

$$\frac{1}{a_0}=|A_0|\left[\frac{\kappa}{2\sqrt{2}\alpha}\right]^{1/2} \tag{42}$$

and the phase variation $\phi(x)$ of the pulse becomes a simple wave number shift given as

$$\phi(x)=-\frac{3\sqrt{2}}{8}|A_0|^2x\ . \tag{43}$$

This compares very favorably with the relations between the soliton parameters as given by Eqs. (5) and (6). The general agreement between the exact soliton curve and the approximate "Gaussian soliton" is also good as is evident from Fig. 5. Finally we note, as a further comparison, that the integral contents under the curves also are very close, viz.,

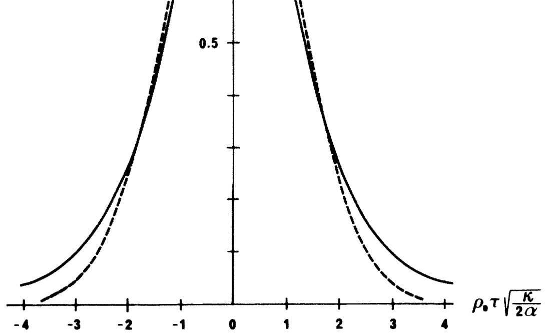

FIG. 5. Comparison between the exact soliton shape (——) given by Eq. (5) and the variationally obtained "Gaussian soliton" (— — —).

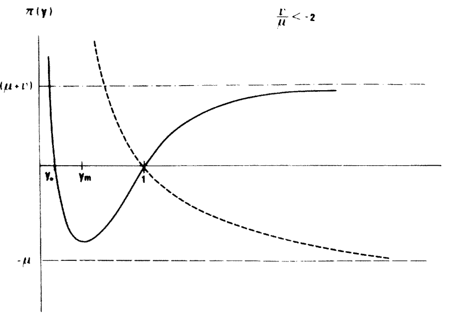

FIG. 6. Qualitative plot of the potential function $\Pi(y)$ in the case of anomalous dispersion and strong nonlinearity ($\nu/\mu<-2$). For comparison the linear case is also inserted (— — —).

$$\frac{\int_{-\infty}^{+\infty}\rho_0\operatorname{sech}(\tau/\tau_b)dt}{\int_{-\infty}^{+\infty}\rho_0\exp(-\tau^2/2a_0^2)dt}=\left[\frac{\pi}{2\sqrt{2}}\right]^{1/2}\simeq1.054\ .$$

This good agreement between the variational solution and the exact nonlinear soliton solution provides a further confirmation of the power of approximation inherent in a variational approach. It is obvious that if we had based our trial functions on hyperbolic secant shaped solutions, the variational procedure would have reproduced the exact soliton solution and instead given a good approximation for the linear Gaussian solution describing the dispersive spreading of an initially Gaussian pulse.

Region IV: $\nu/\mu>-2$ (anomalous dispersion, $\alpha/\kappa>0$, and strong nonlinearity). In this region a potential well is created for values of y less than 1 (see Fig. 6), since $y_*=-(1+\nu/\mu)^{-1}<1$. Thus again, the pulse width will exhibit an oscillatory behavior. However, initially nonlinear effects dominate, and the pulse will start by being compressed to a minimum pulse width a_* given by

$$a_*=\frac{a_0}{|1+\nu/\mu|} \tag{44}$$

before dispersive effects are able to balance the nonlinear compression and make the pulse width increase.

VI. FURTHER COMPARISON WITH SOLITON THEORY

Several of the features of the solutions discussed in the previous section, in particular, for values of the parameter ν/μ in the range $\nu/\mu\le-1$, i.e., regions III and IV, can be related to exact results from soliton theory. In order to make such a comparison, we give some important results for soliton propagation as obtained by inverse-scattering technique and/or numerical solutions of the nonlinear

Schrödinger equation.[3,9] Consider pulses of the form

$$\psi(0,\tau)=f\rho_0 \operatorname{sech}\left[\rho_0\left[\frac{\kappa}{2\alpha}\right]^{1/2}\tau\right], \tag{45}$$

where $f=1$ corresponds to the single soliton solution. Soliton theory predicts that such pulses during propagation will perform a sequence of more or less complicated oscillations in an asymptotic development towards a pure N-soliton solution, where N is determined as the largest integer, which satisfies

$$N\leq f+\tfrac{1}{2}\ . \tag{46}$$

Thus a single soliton solution will eventually appear for all f such that $\frac{1}{2}\leq f\leq\frac{3}{2}$. Furthermore, if we write $f=1+\delta$ ($|\delta|\leq\frac{1}{2}$), the asymptotic value of the pulse amplitude ρ_∞, is given by

$$\rho_\infty=f_\infty\rho_0\ , \tag{47}$$

where

$$f_\infty=1+2\delta \tag{48}$$

and the pulse shape settles down to

$$|\psi_\infty(x,\tau)|=\rho_\infty \operatorname{sech}\left[\rho_\infty\left[\frac{\kappa}{2\alpha}\right]^{1/2}\tau\right]. \tag{49}$$

In connection with these exact results we emphasize the following points obtained from the approximate analysis.

(i) The marginal case, for which nonlinear effects are strong enough to stop the dispersive spreading, is $\nu/\mu=-1$. The corresponding pulse amplitude ρ, for fixed pulse width, is related to the soliton amplitude ρ_s as

$$\rho=\rho_s/\sqrt{2}\ ,$$

which agrees, at least qualitatively with the lower bound amplitude $\rho_s/2$ obtained from soliton theory.

(ii) For $\nu/\mu>-1$ the approximate variational analysis predicts that the amplitude ρ will oscillate as the inverse square root of the pulse width. This implies that ρ will vary between the limits

$$\begin{aligned}&\rho=\rho_0=f\rho_s\ ,\\&\rho=\rho_*=f\rho_s(2f^2-1)^{1/2}\ .\end{aligned} \tag{50}$$

It is instructive to compare these predictions with the results obtained in Ref. 9, where the evolution of pulses of the form given by Eq. (45) was studied for f values in the range $f\sim0.8-1.4$. The pulse amplitude was found to perform a damped oscillatory behavior towards the theoretically predicted asymptotic value determined by Eqs. (47) and (48). We

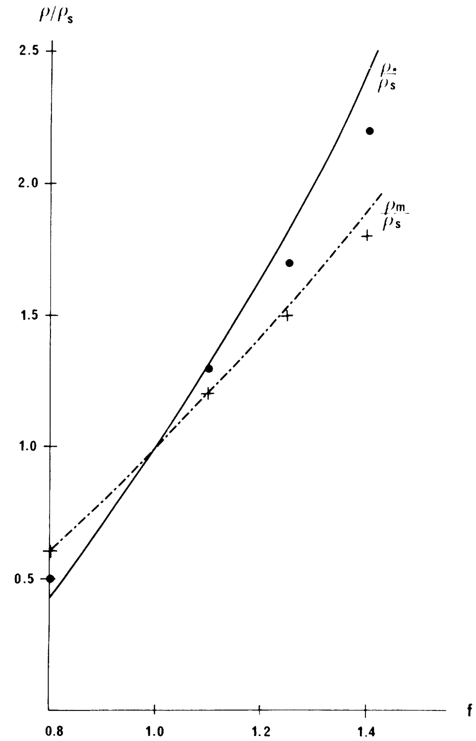

FIG. 7. Comparison between the numerically (Ref. 9) obtained results for peak amplitudes ρ_p (●) and asymptotic amplitudes ρ_∞ (+), and the analytical predictions for ρ_* (——) and $\rho_m\equiv(\rho_0+\rho_*)/2$ (—·—·—·) as given by Eq. (50).

denote the maximum (or in the case $f<1$ the minimum) value of the amplitude in the first oscillation by ρ_p. In Fig. 7 we compare the numerical results for ρ_p (from Ref. 9) with the corresponding analytical prediction for ρ_* as obtained from Eq. (50). The agreement is seen to be quite good.

The variational analysis is unable to account for the damping of the amplitude oscillations. However, the natural choice for the asymptotic amplitude limit would be the arithmetic mean of the upper and lower amplitude bounds. Indeed, as Fig. 7 also shows, the agreement between $\rho_m\equiv(\rho_0+\rho_*)/2$ and ρ_∞ is remarkably good.

VII. DYNAMIC PULSE WIDTH VARIATION

Although a qualitative discussion of the variation of the pulse width was given in the preceding sections, we must solve Eq. (33), with $\Pi(y)$ given by Eq. (34), in order to obtain quantitative information on the dynamical variation of pulse width with distance of propagation. The formal solution of Eq. (33) is obtained as

$$\pm x\sqrt{2}=\int_1^y [(\mu+\nu)y^2-\nu y-\mu]^{-1/2}dy \ . \qquad (51)$$

The explicit solution of Eq. (51) will be of two qualitatively different forms depending on whether $\Pi(y)$ has one or two zeros, i.e., if $\nu/\mu>-1$ or $\nu/\mu<-1$.

A. Case I: $\nu/\mu>-1$ (regions I and II)

In this case the evolution corresponds to a monotonous spreading of the pulse and we obtain the full solution in the implicit form

$$x\sqrt{2\mu}=\frac{1}{\sqrt{1+\xi}}\left[(y-1)\left[y+\frac{1}{1+\xi}\right]\right]^{1/2}+\tfrac{1}{2}\xi(1+\xi)^{-3/2}\ln\frac{2(1+\xi)\left[(y-1)\left[y-\frac{1}{1+\xi}\right]\right]^{1/2}+2(1+\xi)y-\xi}{2+\xi}, \qquad (52)$$

where for convenience we have introduced $\xi=\nu/\mu$. The variation of pulse width, with distance of propagation as determined by Eq. (52), is shown in Fig. 8. For large y, Eq. (52) and Fig. 8 imply an asymptotic straight-line dependence, viz.,

$$y\simeq x[2\mu(1+\xi)]^{1/2}\ , \qquad (53)$$

which reduces to the dispersive result [cf. Eq. (37)] when $\xi=0$.

An important parameter is the characteristic distance x_D required for the pulse width to become twice its initial value. We obtain

$$x_D\sqrt{2\mu}=\frac{(3+2\xi)^{1/2}}{1+\xi}+\frac{\xi}{2}(1+\xi)^{-3/2}\times\ln\frac{2[(1+\xi)(3+2\xi)]^{1/2}+4+3\xi}{2+\xi} \qquad (54)$$

and the variation of x_D with ξ is shown in Fig. 9.

Limit case: $\nu/\mu=-1$. In this limit case the solution becomes especially simple, viz.,

$$\frac{3x}{2}\sqrt{2\mu}=(y+2)\sqrt{y-1}\ . \qquad (55)$$

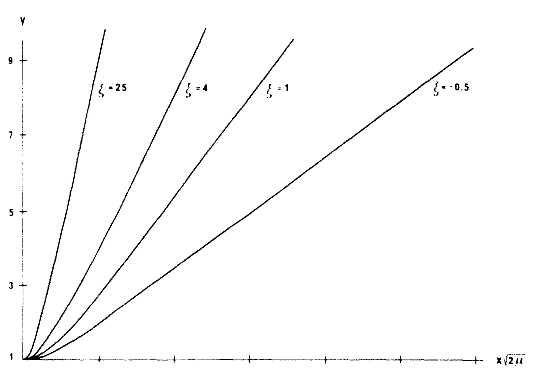

FIG. 8. Variation of pulse width y with distance of propagation x for different ratios of nonlinearity and dispersion as expressed by the parameter $\xi=\nu/\mu>-1$.

Note that asymptotically we obtain [cf. Eq. (53)]

$$y\simeq\left[\frac{3x}{2}\sqrt{2\mu}\right]^{2/3}\ . \qquad (56)$$

B. Case II: $\nu/\mu<-1$ (regions III and IV)

The solution corresponds to an oscillation of the pulse width between the limits $y=1$ and $y=y_*=-(1+\nu/\mu)^{-1}$. Giving only the expressions for the first half cycle we obtain

(a) $-2<\nu/\mu<-1$ (initial pulse spreading):

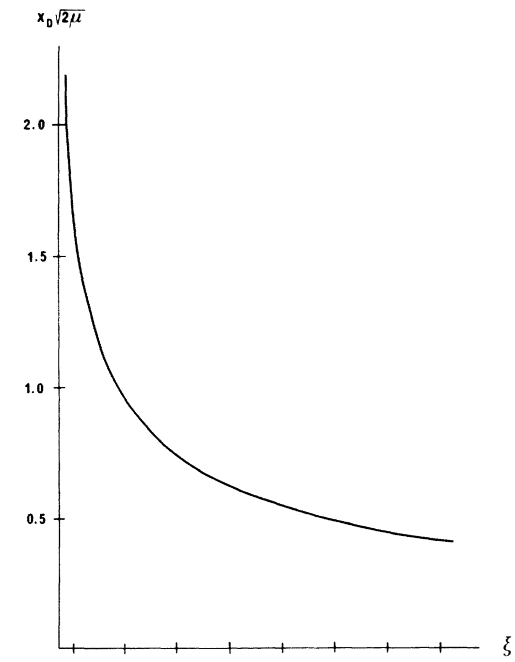

FIG. 9. The variation of x_D with ξ, where x_D is the characteristic distance of propagation at which the pulse width has doubled and $\xi=\nu/\mu$ characterizes the ratio of nonlinearity to dispersion.

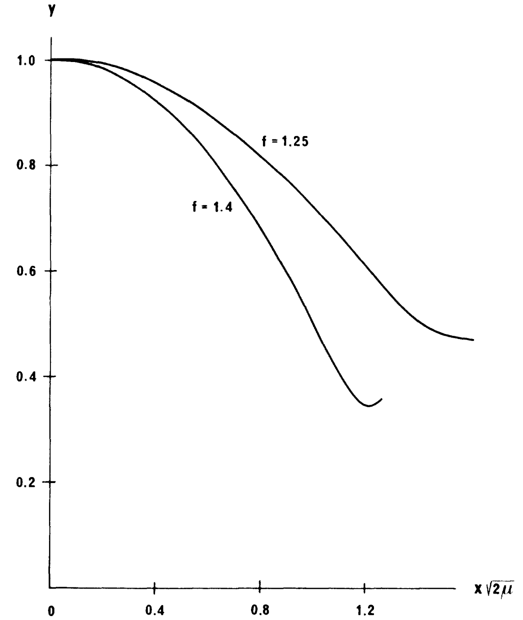

FIG. 10. Variation of pulse width compression factor y with distance of propagation x for two values of initial amplitude, $f=1.25$ and $f=1.4$, respectively.

$$x\sqrt{2\mu}=-\frac{1}{[-(1+\xi)]^{1/2}}\left[(1-y)\left[y+\frac{1}{1+\xi}\right]\right]^{1/2}+\tfrac{1}{2}\xi[-(1+\xi)]^{-3/2}\times\left[\arcsin\frac{2(1+\xi)y-\xi}{2+\xi}-\pi/2\right]. \quad (57)$$

(b) $-2>\nu/\mu$ (initial pulse compression):

$$x\sqrt{2\mu}=\frac{1}{[-(1+\xi)]^{1/2}}\left[(1-y)\left[y+\frac{1}{1+\xi}\right]\right]^{1/2}+\tfrac{1}{2}\xi[-(1+\xi)]^{-3/2}\times\left[\arcsin\frac{2(1+\xi)y-\xi}{2+\xi}-\pi/2\right]. \quad (58)$$

The variation of pulse width with distance of propagation is given in Fig. 10 for initial pulse amplitudes characterized by $f=1.25$ and $f=1.4$, respectively [cf. Eq. (45)]. Since we have already discussed and compared the results for the peak amplitudes and/or pulse compression ratios, the remaining crucial comparison relates to the dynamical period of oscillation. From Eqs. (56) and (57) we obtain the period x_p as

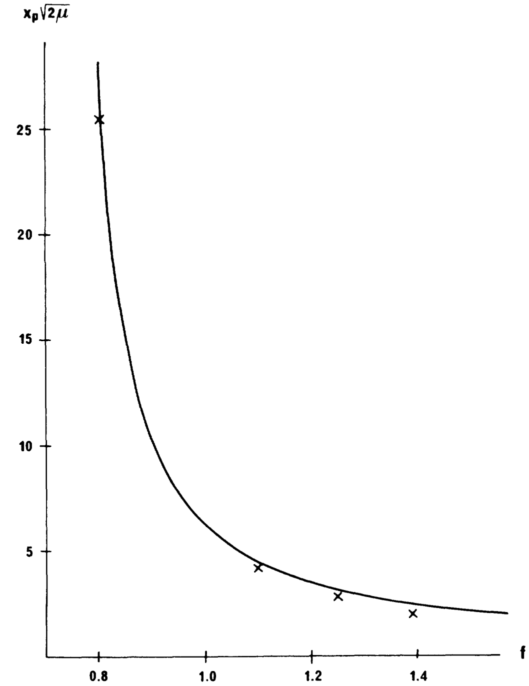

FIG. 11. Comparison between numerically (Ref. 9) obtained results for the period x_p of the amplitude oscillations (×) and the variationally obtained result (——) given by Eq. (60).

$$x_p\sqrt{2\mu}=\frac{\pi|\xi|}{|1+\xi|^{3/2}}. \quad (59)$$

In order to compare with results obtained in Ref. 9, we rewrite Eq. (59) in terms of the factor f [cf. Eq. (45)]

$$x_p\sqrt{2\mu}=\frac{2\pi f^2}{(2f^2-1)^{3/2}}. \quad (60)$$

The period of oscillation x_p as a function of f is shown in Fig. 11, where points corresponding to numerically obtained results (from Ref. 9) are also inserted. The agreement is again very good.

VIII. CONCLUSION

With the present analysis we have demonstrated the possibilities of a variational approach in connection with the nonlinear Schrödinger equation and nonlinear pulse propagation in optical fibers. The main results of the analysis can be summarized as follows:

(i) The potential well description provides a clear and physically suggestive picture of the dynamic balance between nonlinear and dispersive effects. In particular, the qualitative results inferred from the characteristic potential function $\Pi(y)$ are in good agreement with exact results from inverse-scattering theory and/or numerically obtained results.

(ii) Very good quantitative agreement is also found for the evolution of optical pulses, whose initial pulse forms are "close" to the single soliton shape, in the sense discussed in Secs. V and VI. In particular, pulse width, pulse amplitude, and period of amplitude oscillations are found to be in very good agreement with numerically obtained results.

Thus, the present analysis should prove useful, not only as a qualitative approach towards a better physical understanding of the dynamics of nonlinear pulse propagation in optical fibers, but also a quantitative tool, complementary to inverse-scattering theory and numerical analysis.

Finally, we also want to emphasize that the nonlinear Schrödinger equation is truly universal, appearing as it does in almost every field of physics. Thus, the presently obtained results have a much wider area of applicability than simply pulse propagation in optical fibers.

[1]L. F. Mollenauer, R. H. Stolen, and J. P. Gordon, Phys. Rev. Lett. 45, 1095 (1980).
[2]H. Nakatsuka, D. Grischkowsky, and A. C. Balant, Phys. Rev. Lett. 47, 910 (1981).
[3]A. Hasegawa and Y. Kodama, Proc. IEEE 69, 1145 (1981).
[4]A. Hasegawa and Y. Kodama, Opt. Lett. 7, 285, 339 (1982).
[5]D. Grischkowsky and A. C. Balant, Appl. Phys. Lett. 41, 1 (1982).
[6]C. V. Shank, R. L. Fork, R. Yen, R. H. Stolen, and W. J. Tomlinson, Appl. Phys. Lett. 40, 761 (1982).
[7]A. Hasegawa and F. Tappert, Appl. Phys. Lett. 23, 142 (1973); 23, 171 (1973).
[8]B. Niklaus and D. Grischkowsky, Appl. Phys. Lett. 42, 1 (1983).
[9]J. Satsuma and N. Yajima, Prog. Theor. Phys. Suppl. 55, 284 (1974).
[10]D. Anderson and M. Bonnedal, Phys. Fluids 22, 105 (1979).
[11]D. Anderson, M. Bonnedal, and M. Lisak, Phys. Fluids 22, 1839 (1979).